Article

Ag₂O on ZrO₂ as a Recyclable Catalyst for Multicomponent Synthesis of Indenopyrimidine Derivatives

Sandeep V. H. S. Bhaskaruni, Suresh Maddila, Werner E. van Zyl and Sreekantha B. Jonnalagadda *

School of Chemistry & Physics, University of KwaZulu-Natal, Westville Campus, Chiltern Hills, Durban 4000, South Africa; Saisandeep93@gmail.com (S.V.H.S.B.); sureshmskt@gmail.com (S.M.); vanzylw@ukzn.ac.za (W.E.v.Z.)

* Correspondence: jonnalagaddas@ukzn.ac.za; Tel.: +27-31-260-7325; Fax: +27-31-260-3091

check for updates

Abstract: We describe the synthesis of silver loaded on zirconia and its use as an efficient catalyst for a one-pot three-component reaction to synthesize 11 indenopyrimidine derivatives, of which 7 are new compounds. The procedure involves substituted benzaldehydes, indane-1,3-dione, and guanidinium hydrochloride, with ethanol as solvent. The proposed green protocol at room temperature is simple and efficient, giving excellent yields (90–96%) in short reaction times (<30 min). The protocol works well according to the green chemistry principles with respect to high atom economy, no need for column separation, and reusability of the catalyst, which are attractive features. XRD, TEM, SEM, and BET analysis were used to characterize the catalyst materials.

Keywords: indenopyrimidines; no column chromatography; Ag₂O/ZrO₂; heterogeneous catalysis; mixed oxides; green chemistry

1. Introduction

Multicomponent reactions (MCRs) are cherished protocols in organic synthesis due to their vast potential in the fields of medicinal, pharmaceutical, and agro-chemistry [1]. MCRs are different from the other classical synthesis approaches due to their facile synthesis protocols, high atom efficiency, high yields, and minimal by-product formation [2]. Further, the efficacy of MCRs when compared with multistep synthetic protocols lies in the selective formation of several bonds in a single reaction flask with highly desirable yield over a short interval of time [3].

Currently, heterogeneous catalysts play a key role in organic synthesis because they meet most of the goals of green and sustainable chemistry [4]. Researchers have made remarkable improvements in the design of well-defined catalyst materials. Innovative methods have allowed the coherent design and preparation of very active and selective catalyst materials by governing the structure and composition of the active particles [5]. Furthermore, heterogeneous catalysts offer many benefits in synthetic transformations such as outstanding chemical and thermal stability, noncorrosiveness, nonflammability, eco-friendliness, nontoxicity, ease of separation, reusability, and commercial availability [6].

In recent years, zirconium oxide (ZrO₂) have been effusively revealed as a catalyst or a supported catalyst in various potential chemical applications due to its extensive properties such as acidic and basic sites [7], high stability in the presence of redox conditions, active phase support, and chemical consistency related to other supports like alumina and silica. Further, ZrO₂ is low cost, stable, nonhazardous, reusable, and readily available [8]. Silver salts are widely used as catalysts and

their efficacy has been demonstrated in terms of being cost-effective, non-toxic, simple to handle, and appropriate for usage as a one-electron redox system [9]. However, their use in large amounts is unwarranted, but if used in a green-manner as a recyclable catalyst, it has many advantages. Hence, the use of silver-loaded zirconia catalysts is a desirable choice for eco-friendly synthesis.

Among the known heterocyclic compounds, N-heterocyclic scaffolds are very important in medicinal chemistry [10]. In the N-heterocyclic class of scaffolds, pyrimidine and its derivatives play a prominent role [11]. Being the main constituents of several natural products, these pyrimidines represent a significant class of molecules which have been of increased interest in recent years owing to their valuable pharmacological and biological applications in antimicrobial [12], antifungal [13], anti-tumor [14], anti-HIV [15], anti-tubercular [16], anti-inflammatory [17], and antimalarial [18] activities. Moreover, aryl-indenopyrimidines have been used as adenosine A2A receptor antagonists [19], which are useful, and many reports have dealt with the preparation of different types of pyrimidine derivatives via multicomponent reactions. Owing to their economic viability and scientific importance, methodologies have been described for the synthesis of various types of substituted pyrimidines. Diverse catalytic systems such as NaOH, references [20–22] sodium methoxide [23], 1-sulfonic acid-3-methyl imidazolium ferric chloride/NaY [24], α-Fe_2O_3-MCM-41-P [25], and uranyl acetate/succinimide sulfonic acid [26] have been used in the synthesis of pyrimidine derivatives. However, these protocols invariably demand expensive reagents, high energy input, and lengthy reaction times. Other limitations are lower yields and the need for solvents and column separations. There is, thus, a demand for a greener preparation method for indenopyrimidines. We found no literature reports to date using metal complexes or metal oxides as catalysts in their synthesis. Although silver-loaded ZrO_2 have been reported as a catalyst for varied reactions [27,28], no protocols have been described for the synthesis of indenopyrimidines via MCRs.

We recently reported several green synthetic approaches of various medicinally interesting heterocyclic scaffolds [29–37]. Encouraged by those favorable results with different substituted heterocyclic scaffolds, here we describe the synthesis and characterization of silver loaded on zirconia and its efficiency in the one-pot synthesis of functionalized indenopyrimidines via a three-component reaction at room temperature (RT).

2. Experimental Section

2.1. Catalyst Preparation

Supported catalysts with different wt % (weight percentage) of silver-loaded zirconia (1, 2.5, and 5.0 wt %) were synthesized following a wet impregnation process [38,39]. The solid heterogeneous catalyst was prepared by combining zirconia (ZrO_2, 3 g, Alfa Aesar, Ward Hill, MA, USA) and a suitable quantity of silver chloride ($AgCl_2$, Alfa Aesar) dissolved in distillated water (60 mL). The mixture was stirred at room temperature (RT) for 5–7 h. After this time, the ensuing slurry was filtered under vacuum. It was dried in an oven at 120–130 °C for 6 h and calcined in the presence of air at 450 °C for 5 h to afford the (1.0, 2.5, and 5.0 wt %) silver on zirconia.

2.2. General Procedure for the Synthesis of Indenopyrimidine Derivatives

In a typical reaction, an equimolar mixture of aldehydes (1 mmol), indane-1,3-dione (1 mmol), and guanidinium hydrochloride (1 mmol) were dissolved in ethanol (5 mL) at RT, followed by the addition of Ag_2O–ZrO_2 (60 mg) as a catalyst. The reaction mixture was held at RT for 30 min under stirring (Scheme 1), while the reaction progress was monitored by TLC at regular time intervals. When the reaction was complete, the mixture was filtered, and ethyl acetate was used to extract the filtrate which was then evaporated under reduced pressure to obtain the crude product and washed with ethanol. The reaction product was recrystallized in ethanol to obtain the pure target compound. The yields reported are the weighed values after recrystallization and isolation. The products were

further characterized by ^{1}H-NMR, ^{13}C-NMR, HRMS, and FT-IR analysis. The related details and spectra are given in the Supplementary Information File (SI-II & III).
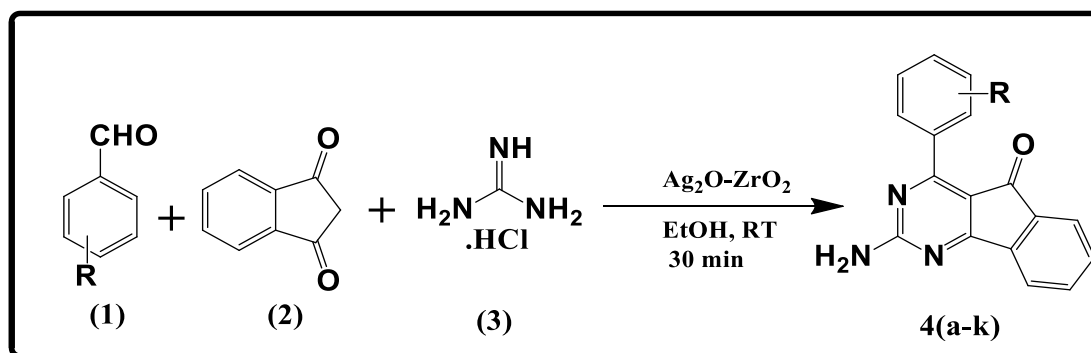
Scheme 1. Synthesis of novel indenopyrimidine derivatives. RT = room temperature.

2-Amino-4-(2-methoxyphenyl)-5H-indeno[1,2–d]-pyrimidine-5-one (**4a**). ^{1}H-NMR (DMSO-d_6, 400 MHz) δ = 3.83 (s, 3H, -OCH$_3$), 7.09 (d, *J* = 7.6 Hz, 1H, Ar-H), 7.16 (d, *J* = 8.16 Hz, 1H, Ar-H), 7.61 (t, *J* = 1.2 Hz, 1H, Ar-H), 7.92–7.95 (m, 4H, Ar-H), 8.22 (s, 2H, -NH$_2$), 8.77–8.79 (m, 1H, Ar-H). ^{13}C-NMR δ = 56.03, 111.56, 120.10, 121.00, 122.94, 122.98, 128.16, 133.09, 135.69, 135.78, 135.86, 138.96, 139.32, 141.79, 160.05, 188.50, 189.61; FT-IR: 3269.10 (-NH), 2957.02 (-CH), 1710 (-C=O), 1593.28 (-C=C), 1483.73 (-C=N), 733.81 (-CH).

2-Amino-4-(4-methoxyphenyl)-5H-indeno[1,2-d]-pyrimidine-5-one (**4b**). ^{1}H-NMR (DMSO-d_6, 400 MHz) δ = 3.89 (s, 3H, -OCH$_3$), 7.13 (d, *J* = 8.92 Hz, 2H, Ar-H), 7.80 (s, 2H, -NH$_2$), 7.71 (s, 2H, NH$_2$), 7.93–7.95 (m, 4H, Ar-H), 8.60 (d, *J* = 8.92 Hz, 2H, Ar-H). ^{13}C-NMR δ = 55.72, 114.49, 122.86, 125.86, 126.28, 135.54, 135.69, 136.98, 139.27, 141.69, 145.72, 163.77, 188.96, 189.80; FT-IR: 3010.13 (-NH), 2941.01 (-CH), 1712.14 (-C=O), 1673.42 (-C=C), 1468.81 (-C=N), 771.95 (-CH); HRMS of [C$_{18}$H$_{13}$N$_3$O$_2$ + H]$^+$ (*m/z*): 304.0766; Calcd: 304.0763.

2-Amino-4-(2,3-dimethoxyphenyl)-5H-indeno[1,2-d]-pyrimidine-5-one (**4c**). ^{1}H-NMR (DMSO-d_6, 400 MHz) δ = 3.91 (s, 6H, -OCH$_3$), 7.21 (t, *J* = 8.08 Hz, 1H, Ar-H), 7.32–7.34 (m, 1H, Ar-H), 7.94–8.14 (m, 4H, Ar-H), 8.36 (s, 2H, -NH$_2$), 8.38 (t, *J* = 1.04 Hz, 1H, Ar-H). ^{13}C-NMR δ = 55.95, 61.49, 118.22, 123.05, 123.10, 123.61, 124.23, 126.21, 129.53, 136.02, 139.00, 139.42, 141.89, 150.23, 152.19; FT-IR: 3087.99 (-NH), 2939.24 (-CH), 1711.98 (-C=O), 1673.55 (-C=C), 1469.79 (-C=N), 771.94 (-CH); HRMS of [C$_{19}$H$_{15}$N$_3$O$_3$ + H]$^+$ (*m/z*): 334.0992; Calcd: 334.1008.

2-Amino-4-(2,5-dimethoxyphenyl)-5H-indeno[1,2-d]-pyrimidine-5-one (**4d**). ^{1}H-NMR (DMSO-d_6, 400 MHz) δ = 3.82 (s, 3H, -OCH$_3$), 3.89 (s, 3H, -OCH$_3$), 7.11 (d, *J* = 9.12 Hz, 1H, Ar-H), 7.21 (d, *J* = 3.12 Hz, 1H, Ar-H), 7.93–7.97 (m, 4H, Ar-H), 8.23 (s, 2H, -NH$_2$), 8.64 (d, *J* = 3.2 Hz, 1H, ArH). ^{13}C-NMR δ = 55.51, 56.38, 112.72, 116.49, 121.32, 123.07, 128.11, 135.75, 135.89, 138.84, 139.29, 141.87, 152.29, 154.92, 188.82, 189.64, 206.58; FT-IR: 3087.87 (-NH), 2950.12 (-CH), 1746.67 (-C=O), 1683.90 (-C=C), 1588.60 (-C=N), 780.18 (-CH); HRMS of [C$_{19}$H$_{15}$N$_3$O$_3$ + H]$^+$ (*m/z*): 334.0434; Calcd: 334.0441.

2-Amino-4-(2-bromophenyl)-5H-indeno[1,2-d]-pyrimidine-5-one (**4e**). ^{1}H-NMR (DMSO-d_6, 400 MHz) δ = 7.52–7.59 (m, 2H, NH$_2$), 7.89–7.98 (m, 7H, Ar-H), 8.00 (s, 1H, Ar-H). ^{13}C-NMR δ = 122.83, 122.91, 124.36, 130.67, 132.12, 132.32, 135.70, 135.92, 140.42, 141.20, 141.35, 141.67, 142.03, 142.98, 197.19, 198.68; FT-IR: 3089.08 (-NH), 2941.43 (-CH), 1745.65 (-C=O), 1673.02 (-C=C), 1564.46 (-C=N), 771.47 (-CH), 619.03 (-C-Br); HRMS of [C$_{17}$H$_{10}$BrN$_3$O + H]$^+$ (*m/z*): 353.1042; Calcd: 353.1042.

2-Amino-4-(2-fluorophenyl)-5H-indeno[1,2-d]-pyrimidine-5-one (**4f**). ^{1}H-NMR (DMSO-d_6, 400 MHz) δ = 7.39 (s, 1H, NH$_2$), 7.68 (t, *J* = 1.08 Hz, 2H, Ar-H), 7.92–7.99 (m, 6H, Ar-H). ^{13}C-NMR δ = 115.65, 115.86, 123.24, 124.49, 124.52, 133.07, 136.07, 136.21, 139.60, 141.99, 160.66, 188.07, 188.85, 197.56, 198.69;

FT-IR: 3275.94 (-NH), 2956.87 (-CH), 1740.56 (-C=O), 1620.19 (-C=C), 1485.01 (-C=N), 1008.10 (-C-F), 757.33 (-CH); HRMS of $[C_{17}H_{10}BrN_3O + H]^+$ (*m/z*): 292.0732; Calcd: 292.0732.

2-Amino-4-(3,4-dimethoxyphenyl)-5H-indeno[1,2-d]-pyrimidine-5-one (**4g**). ^{1}H-NMR (DMSO-d_6, 400 MHz) δ = 3.90 (d, *J* = 3.84 Hz, 6H, -OCH$_3$), 7.16 (d, *J* = 8.52 Hz, 1H, Ar-H), 7.80 (s, 1H, NH$_2$), 7.92–7.97 (m, 4H, Ar-H), 8.02–8.04 (m, 1H, Ar-H), 8.68 (d, *J* = 1.92 Hz, 1H, ArH). ^{13}C-NMR δ = 55.18, 111.53, 115.74, 122.78, 122.91, 126.09, 131.08, 135.56, 135.69, 139.22, 146.43, 148.31, 153.91, 189.85; FT-IR: 3088.10 (-NH), 2942.06 (-CH), 1712.66 (-C=O), 1673.31 (-C=C), 1468.88 (-C=N), 772.61 (-CH), 801.96 (-CH).

2-Amino-4-(3-hydroxyphenyl)-5H-indeno[1,2-d]-pyrimidine-5-one (**4h**). ^{1}H-NMR (DMSO-d_6, 400 MHz) δ = 7.01–7.04 (m, 1H, Ar-H), 7.35 (t, *J* = 7.88 Hz, 1H, Ar-H), 7.71 (s, 2H, NH$_2$), 7.82 (d, *J* = 7.72 Hz, 1H, Ar-H), 7.92–7.96 (m, 5H, Ar-H), 9.86 (s, 1H, -OH). ^{13}C-NMR δ = 119.61, 120.67, 123.00, 123.04, 125.46, 128.94, 129.69, 133.84, 135.77, 135.93, 139.33, 141.89, 145.82, 157.33, 188.45, 189.43; FT-IR: 3241.25 (-OH), 3088.13 (-NH), 1745.77 (-C=O), 1665.42 (-C=C), 1484.83 (-C=N), 780.62 (-CH); HRMS of $[C_{17}H_{11}N_3O_2 + H]^+$ (*m/z*): 290.0732; Calcd: 290.0732.

2-Amino-4-(4-bromophenyl)-5H-indeno[1,2-d]-pyrimidine-5-one (**4i**). ^{1}H-NMR (DMSO-d_6, 400 MHz) δ = 7.77 (d, *J* = 8.52 Hz, 2H, Ar-H), 7.81 (s, *J* = 8.56 Hz, 2H, -NH$_2$), 7.95–7.99 (m, 4H, Ar-H), 8.41 (d, *J* = 8.52 Hz, 2H, Ar-H). ^{13}C-NMR δ = 103.27, 109.58, 110.67, 112.60, 116.48, 136.51, 143.42, 151.63, 151.95, 152.67, 167.34, 194.19; FT-IR: 3087.96 (-NH), 1724.92 (-C=O), 1685.17 (-C=C), 1485.31 (-C=N), 828.42 (-CH), 606.46 (-C-Br).

2-Amino-4-(4-chlorophenyl)-5H-indeno[1,2-d]-pyrimidine-5-one (**4j**). ^{1}H-NMR (DMSO-d_6, 400 MHz) δ = 7.36 (d, *J* = 8.52 Hz, 2H, -NH$_2$), 7.64 (d, *J* = 8.56 Hz, 1H, Ar-H), 7.85–7.97 (m, 6H, Ar-H), 7.82 (d, *J* = 7.72 Hz, 1H, Ar-H), 8.51 (d, *J* = 8.6 Hz, 1H, Ar-H). ^{13}C-NMR δ = 122.57, 122.79, 123.13, 127.74, 127.82, 128.85, 130.79, 135.36, 135.59, 137.85, 141.51, 143.73, 197.94, 198.14, 199.07; FT-IR: 3089.02 (-NH), 1712.07 (-C=O), 1673.33 (-C=C), 1469.06 (-C=N), 802.02 (-CH), 702.10 (-C-Cl); HRMS of $[C_{17}H_{10}ClN_3O + H]^+$ (*m/z*): 308.1139; Calcd: 308.114.

2-Amino-4-(4-ethylphenyl)-5H-indeno[1,2-d]-pyrimidine-5-one (**4k**). ^{1}H-NMR (DMSO-d_6, 400 MHz) δ = 1.22 (t, *J* = 7.56 Hz, 3H, -CH$_3$), 2.68–2.79 (m, 2H, -CH$_2$), 7.42 (d, *J* = 8.2 Hz, 2H, Ar-H), 7.83 (s, 2H, -NH$_2$), 7.93–7.96 (m, 4H, Ar-H), 8.46 (d, *J* = 8.24 Hz, 2H, Ar-H). ^{13}C-NMR δ = 15.03, 28.42, 30.63, 122.56, 122.98, 123.04, 128.30, 130.48, 134.22, 135.57, 135.75, 135.90, 139.39, 141.86, 142.99, 145.64, 150.32, 188.69, 189.56, 206.47; FT-IR: 3088.40 (-NH), 2941.60 (-CH), 1712.33 (-C=O), 1673.31 (-C=C), 1469.87 (-C=N), 802.02 (-CH).

3. Results and Discussion

3.1. Crystallinity by Powder XRD (PXRD) Studies

Figure 1 illustrates the crystalline phases of calcined silver oxide–zirconia catalyst material. The PXRD patterns of the catalytic sample display the major 2θ peak values at 24.2°, 28.2°, 31.3°, 35.4°, 40.5°, 45.0°, 50.3°, 55.4°, and 60.1° corresponding to zirconia; the peak values were correlated with the international standard file (JCPDS file no. 37-1484). In addition, the catalyst material revealed diffraction patterns at 2θ angles of 38.1°, 44.3°, 64.4°, and 77.4° corresponding to the Ag$_2$O (JCPDS file no 72-2108). The peaks recognized in the diffractogram indicate the polycrystalline nature of the catalyst materials. Further, the average crystallite size of the catalyst was measured by the Debye–Scherrer formula using the strongest maximum-intensity diffraction peak, about 9.2 nm for 2.5% Ag$_2$O/ZrO$_2$.
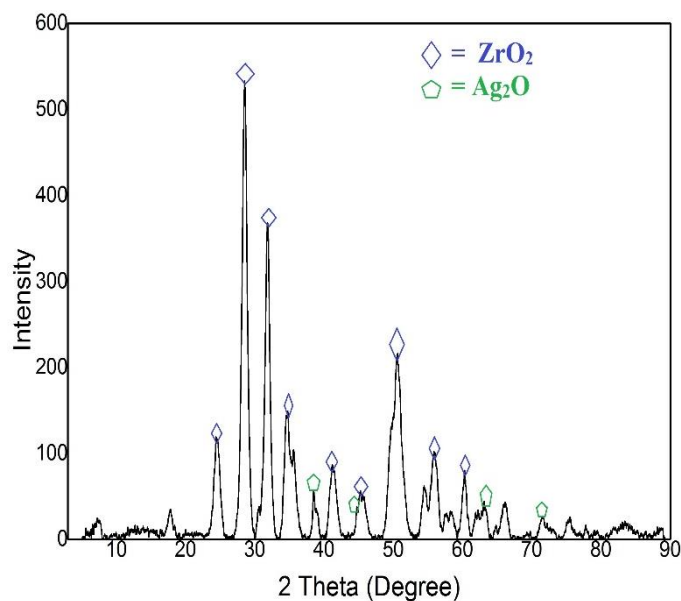
Figure 1. Powder X-ray diffractogram of 2.5% Ag$_2$O–ZrO$_2$ catalyst.

3.2. TEM Analysis

The transition electron microscopy images (Figure 2) provide the morphology of prepared Ag$_2$O/ZrO$_2$ of different wt %. In this image, the silver oxide particle dimensions are mostly in the range between 10 and 16 nm, with black spherical shapes and seemingly well distributed. Further, zirconia is revealed as white globular-shaped particles. It is clearly observed that 1% has a lesser dispersion of Ag, whereas 5% has more Ag agglomerated on the surface of Zr, which fails to provide more active sites to facilitate the reaction. Changes in the morphology of the recovered catalyst after reaction were marginal.
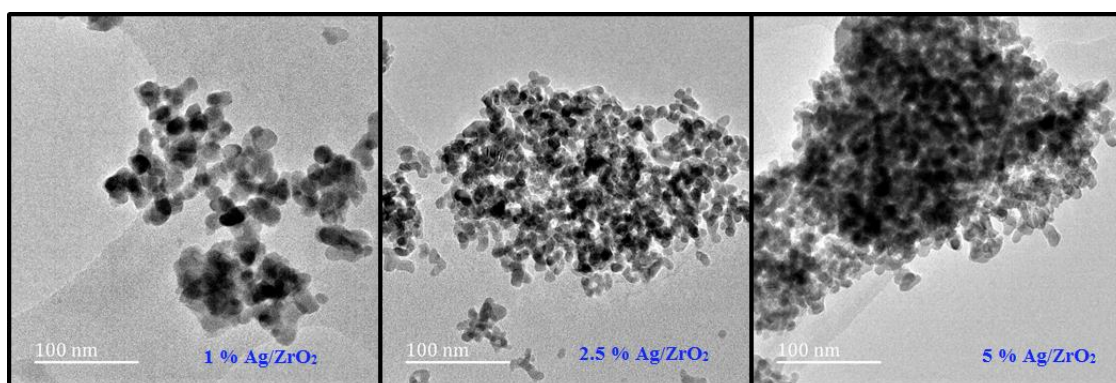

Figure 2. TEM micrographs of 1%, 2.5%, and 5% Ag$_2$O–ZrO$_2$ catalyst.

3.3. SEM Analysis

The morphology and size dispersion of the catalyst material were determined with SEM analysis. In Figure 3, a large number of white and irregular shapes are observed for 2.5% Ag$_2$O loaded on ZrO$_2$. Small silver oxide particles were revealed as white irregular aggregates on the zirconia surface. The micrographs from SEM–EDX validate the even distribution of silver oxide on the zirconia surface. Results also confirm the data from ICP elemental analysis. The mapping also shows the presence of Ag on ZrO$_2$. Furthermore, the morphology of the catalyst from the SEM images also shows the crystallinity and homogeneity of the sample.
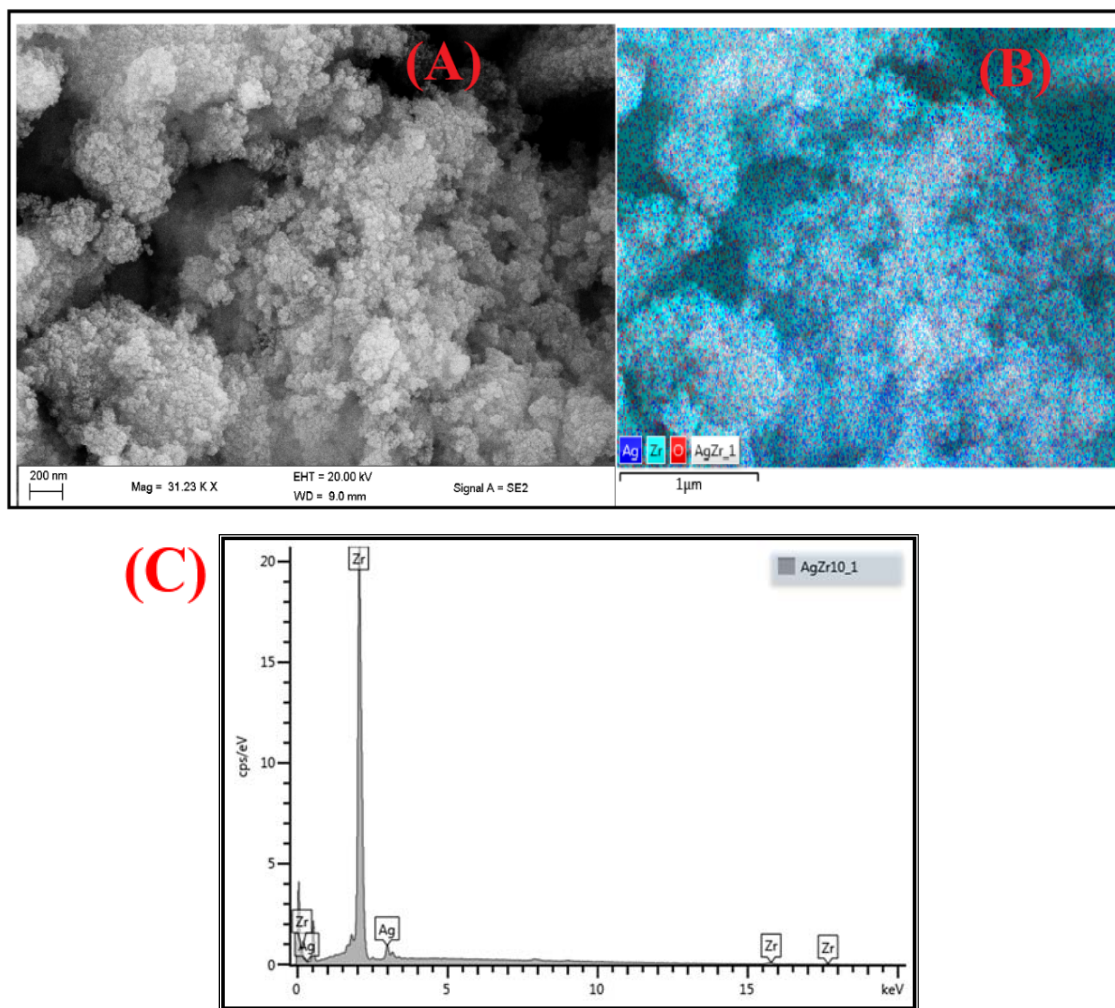
Figure 3. (**A**) SEM micrograph; (**B**) SEM mapping; (**C**) EDS spectra of 2.5% Ag$_2$O–ZrO$_2$ catalyst.

3.4. BET Surface Area Analysis

The nitrogen adsorption/desorption isotherm and resulting pore size dispersion of the 2.5% Ag$_2$O/ZrO$_2$ catalyst material is shown in Figure 4. The catalyst material exhibits a type IV isotherm with the presence of a typical H2 hysteresis loop, which designates the mesoporous nature of the material as per the IUPAC classification. The Barrett-Joyner-Halenda (BJH) pore size distribution describes a mesoporous texture for the material, and the isotherm P/Po range was 0.61–0.98. The BET surface area was measured at 89.52 m^2/g with a pore volume of 0.330 cm^3/g and pore size of 10.3 nm. The ICP study indicates the presence of >1.98 wt % of silver in the catalyst material.

3.5. Pyridine Adsorbed FT-IR Spectroscopy

The nature of acidic sites on the 2.5% Ag$_2$O-loaded ZrO$_2$ surface was examined by employing ex situ pyridine FT-IR spectroscopy (Figure 5) [40]. Infrared (IR) spectra were recorded on a Perkin Elmer Precisely equipped with a Universal ATR sampling accessory using a diamond crystal. The powdered material was placed on the crystal and a force of 120 psi was applied to ensure proper contact between the material and the crystal. The spectra were analyzed using Spectrum 100 software. Before recording the IR spectra, pyridine was adsorbed by placing a drop of pyridine on 10 mg of the sample followed by evacuation in air for 1 h at room temperature to remove reversibly adsorbed pyridine on the surface of the catalyst. The IR band at 1540 cm^{-1} confirmed the presence of Brønsted acidic sites (B). The peak observed at 1485 cm^{-1} is attributed to both Brønsted and Lewis acidic sites (B + L). The prominent

absorption band at 1450 cm^{-1} is due to the pyridine adsorbed on Lewis acidic sites (L) of the catalyst. The presence of more Lewis acidic sites on the catalyst surface than Brønsted acidic sites is shown in Figure 5. Generally, more Lewis acidic sites are anticipated in the Ag$_2$O–ZrO$_2$ catalyst due to the availability of vacant metal orbitals on the surface of the catalyst, which are capable of accepting electron pairs from the electron-rich species [41]. Except for the assigned peaks, the other IR bands are mostly less intensive, mainly due to the signal-to-noise ratio, which was unavoidable.
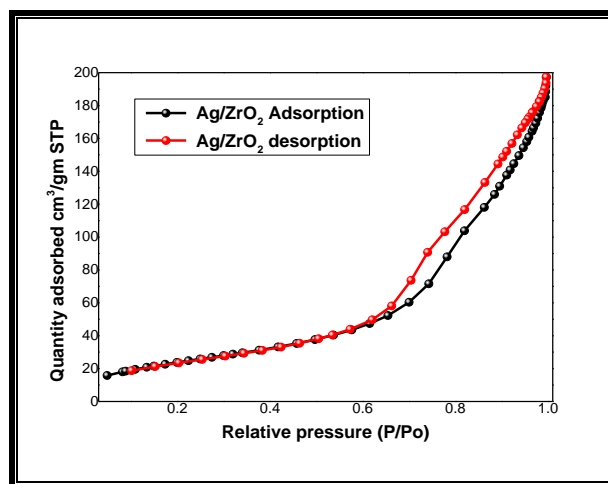

Figure 4. N$_2$ adsorption–desorption isotherms of 2.5% Ag$_2$O–ZrO$_2$ catalyst.

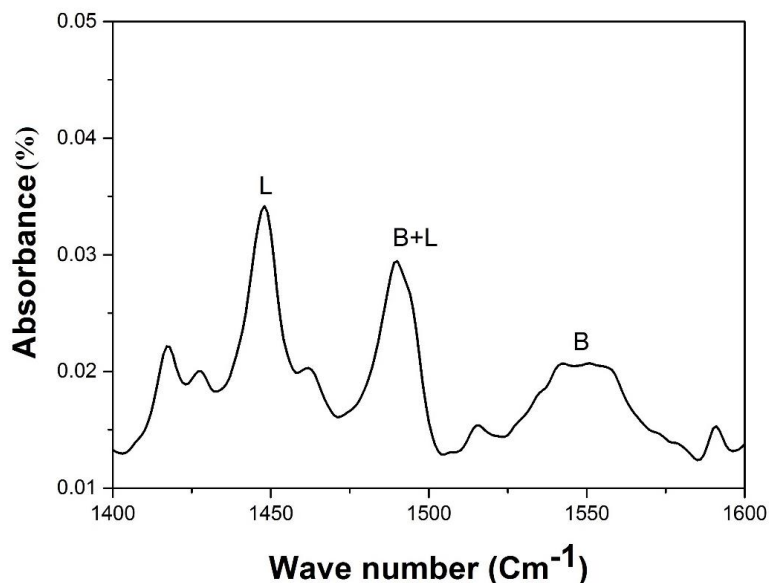**Figure 5.** Pyridine FT-IR spectra of 2.5% Ag$_2$O/ZrO$_2$ catalyst. B = Brønsted acidic sites; L = Lewis acidic sites; B + L = Brønsted and Lewis acidic sites.

4. Reaction Optimization

For optimization of the reaction conditions for a one-pot, three-component reaction involving 2-methoxy benzaldehyde (1 mmol), indane-1,3-dione (1 mmol), and guanidinium hydrochloride (1 mmol), various reaction conditions such as effect of temperature, solvents, and catalysts were investigated. In the absence of solvent and catalyst, no product occurred at RT or under reflux conditions, even after 10 h of reaction (Table 1, entries 1 and 2). The reaction was carried out in ethanol in the presence of various basic catalysts like TEA, pyridine, NaOH, and K$_2$CO$_3$ at RT;

only trace amounts of material were obtained (Table 1, entries 3–6). Reactions with ionic liquids such as (Bmim) BF$_4$ or L-proline (Table 1, entries 7 and 8) as a catalyst gave low yields. When the reaction was conducted using acidic catalysts such as AcOH, FeCl$_3$, and PTSA, moderate yields of product were attained after 4 h (Table 1, entries 9–11). Consequently, reaction was attempted in presence of pure metal oxide catalysts, such as SiO$_2$, ZrO$_2$, and Al$_2$O$_3$, and the reaction showed good yields after 2.0–3.0 h reaction time (Table 1, entries 12–14). Based on the promising outcome with zirconia oxide, to enhance the reaction performance, the efficiencies of different metal oxides loaded on zirconia, such as 2.5% CuO/ZrO$_2$, MnO$_2$/ZrO$_2$, and Ag$_2$O/ZrO$_2$, were examined. These mixed-oxide heterogeneous catalysts gave very good to excellent yields (82–96%) (Table 1, entries 15–17), while the best result was obtained with Ag$_2$O/ZrO$_2$ (96% yield, 30 min). Bimetallic metal oxides showed higher activity than their parent metal oxides, presumably due to a better distribution of the active metal on the support and the synergistic activity between the loaded and support materials, providing optimum distribution and increased number of active sites compared to their oxide homologues.

Table 1. Effect of catalysts on the synthesis of **4a** [a].

Entry	Catalyst	Solvent	Condition	Time (h)	Yield (%) [b]
1	–	–	RT	10	–
2	–	–	Reflux	10	–
3	TEA	EtOH	RT	8.0	9
4	Pyridine	EtOH	RT	8.5	13
5	NaOH	EtOH	RT	7.5	25
6	K$_2$CO$_3$	EtOH	RT	7.0	19
7	(Bmim)BF$_4$	EtOH	RT	10	23
8	L-proline	EtOH	RT	10	27
9	AcOH	EtOH	RT	5.0	43
10	FeCl$_3$	EtOH	RT	4.5	50
11	PTSA	EtOH	RT	5.0	45
12	SiO$_2$	EtOH	RT	2.5	62
13	ZrO$_2$	EtOH	RT	2.0	79
14	Al$_2$O$_3$	EtOH	RT	3.0	59
15	2.5% CuO/ZrO$_2$	EtOH	RT	1.5	82
16	2.5% MnO$_2$/ZrO$_2$	EtOH	RT	1.0	87
17	2.5% Ag$_2$O/ZrO$_2$	EtOH	RT	0.20	96

[a] All products were characterized by ^{1}H-NMR, ^{13}C-NMR, HRMS, and FT-IR spectral analysis. [b] Isolated yields after recrystallization. – No reaction.

The effect of solvents on the title reaction was investigated in the presence of varied nonpolar solvents. No reaction occurred in n-hexane or toluene. When the reaction was performed in polar aprotic solvents such as THF, DMF, and MeCN, the yield of product was low. In the polar protic solvent MeOH, the yield was good, but lower than that with EtOH. Hence, EtOH was chosen as the solvent for the remainder of the studies. The optimized results are shown in Table 2 (entries 1–8).

Table 2. Optimization of various solvent conditions for the model reaction [a].

Entry	Solvent	Time (min)	Yield (%)
1	No solvent	120	–
2	n-hexane	120	–
3	toluene	90	–
4	THF	75	10
5	DMF	65	18
6	MeCN	60	25
7	MeOH	45	81
8	EtOH	30	96

[a] Reaction conditions: arylaldehyde (**1**), (1 mmol), 1,3-Indandione (1 mmol) (**2**), and guanidinium hydrochloride (**3**) (1 mmol) and solvent (5 mL) were stirred at room temperature. – No isolated yields.

Assuming silver oxide loaded on zirconia as the ideal model catalyst, the contribution of % silver loading on zirconia was investigated at 1.0%, 2.5%, and 5.0% Ag_2O/ZrO_2. While 1% Ag loading gave a 90% yield in 45 min, relative to the 2.5% Ag, the 5% Ag neither improved the yield nor decreased the reaction time. The best activity was observed with 2.5% Ag_2O/ZrO_2; hence, this was taken as the optimum loading. This could be due to the optimum dispersion of Ag_2O on ZrO_2, when compared to 5% $Ag_2O//ZrO_2$, where dispersion was less uniform due to the possible aggregation of silver particles. Hence, catalytic activity was lower compared to the 2.5% loading. The 2.5% loading recorded greater activity than 1% $Ag_2O//ZrO_2$. Possibly, the former had more active sites than the latter (Figure 2). A discussion on the role of the Lewis acidic sites in the reaction is part of the mechanism section (Scheme 2). The efficacy of the reaction, including yield and reaction times for 2.5 wt % Ag_2O/ZrO_2, is summarized in Table 3. An increase in catalyst amount from 20 mg to 60 mg improved the yield from 52% to 96% and reduced the reaction time. The increase in the product may be attributed to the comparative increase in the number of available active sites, possibly accelerating the reaction. An increase in the amount of catalyst from 60 mg to 120 mg registered no significant change in the yield of product or reaction time. Hence, 60 mg of the catalyst was considered the ideal amount for the chosen synthesis.

Table 3. Optimization of various weight % for the model reaction with 2.5% Ag_2O/ZrO_2 catalyst [a].

Entry	Catalyst (mg)	Time (min)	Yield (%)
1	20	100	56
2	40	50	79
3	60	30	96
4	80	30	96
5	100	30	96
6	120	40	96

[a] Reaction conditions: arylaldehyde (**1**) (1 mmol), 1,3-indanedione (**2**) (1 mmol), and guanidine hydrochloride (**3**) (1 mmol) and catalyst and solvent (5 mL) were stirred at room temperature.

Encouraged by the results, we further explored the applicability of the protocol for other substituted aldehydes under the optimized reaction conditions, by using 10 other substituted aldehydes. The corresponding indenopyrimidines afforded excellent yields in similar reaction times (30 min) (Table 4, entries 1–11). All the reactions, irrespective of electron-withdrawing or electron-donating groups at ortho, meta, or para positions, generally gave excellent yields. All the product molecules were fully characterized by employing ^{1}H-NMR, ^{13}C-NMR, FT-IR, and HRMS spectral analysis.

Table 4. Synthesis of novel functionalized pyridine derivatives by 2.5% Ag_2O/ZrO_2 catalyst [a].

Entry	R	Product	Yield * (%)	m.p. (°C)	Lit. m.p. (°C)
1	2-OMe	**4a**	94	119–121	-
2	4-OMe	**4b**	93	136–137	100 [20]
3	2,3-(OMe)$_2$	**4c**	94	183–184	-
4	2,5-(OMe)$_2$	**4d**	92	200–201	-
5	2-Br	**4e**	94	197–198	-
6	2-F	**4f**	92	239–241	-
7	3,4-(OMe)$_2$	**4g**	96	176–178	178 [20]
8	3-OH	**4h**	95	246–248	-
9	4-Br	**4i**	94	221–223	210 [20]
10	4-Cl	**4j**	90	239–241	244 [20]
11	4-Et	**4k**	94	204–206	-

[a] Reaction conditions: arylaldehyde (**1**) (1 mmol), 1,3-indanedione (**2**) (1 mmol), and guanidine hydrochloride (**3**) (1 mmol), catalyst (60 mg), and ethanol solvent (5 mL) were stirred at room temperature. R = substituted benzaldehydes. - New compounds/no literature (lit.) data. * = Isolated yields after recrystallization.

A proposed mechanism for the one-pot three-component reaction is outlined in Scheme 2. The presence of Lewis acidic sites on the catalyst surface facilitates the reactants to undergo reaction in a shorter time. It is assumed that in the first step, the Lewis acidic sites with the carbonyl oxygen generate the carbonium ion (**a**) [42]. In a fast reaction with the carbonium ion, the active methylene group affords intermediate (**b**), which desorbs from the catalyst surface by abstracting a proton from the protic solvent, EtOH (**b**), to form (**c**). On further dehydration (**c**), it produces the condensation product (**A**). Next, a Michael addition occurs between the intermediate (**A**) and the guanidinium, followed by cyclization and aromatization, and the transient intermediate yields the target compound—the substituted pyrimidine-5-one derivative. The catalytic efficiency of the Ag_2O/ZrO_2 on the title reaction in comparison with other reported catalysts is summarized in the Table 5.
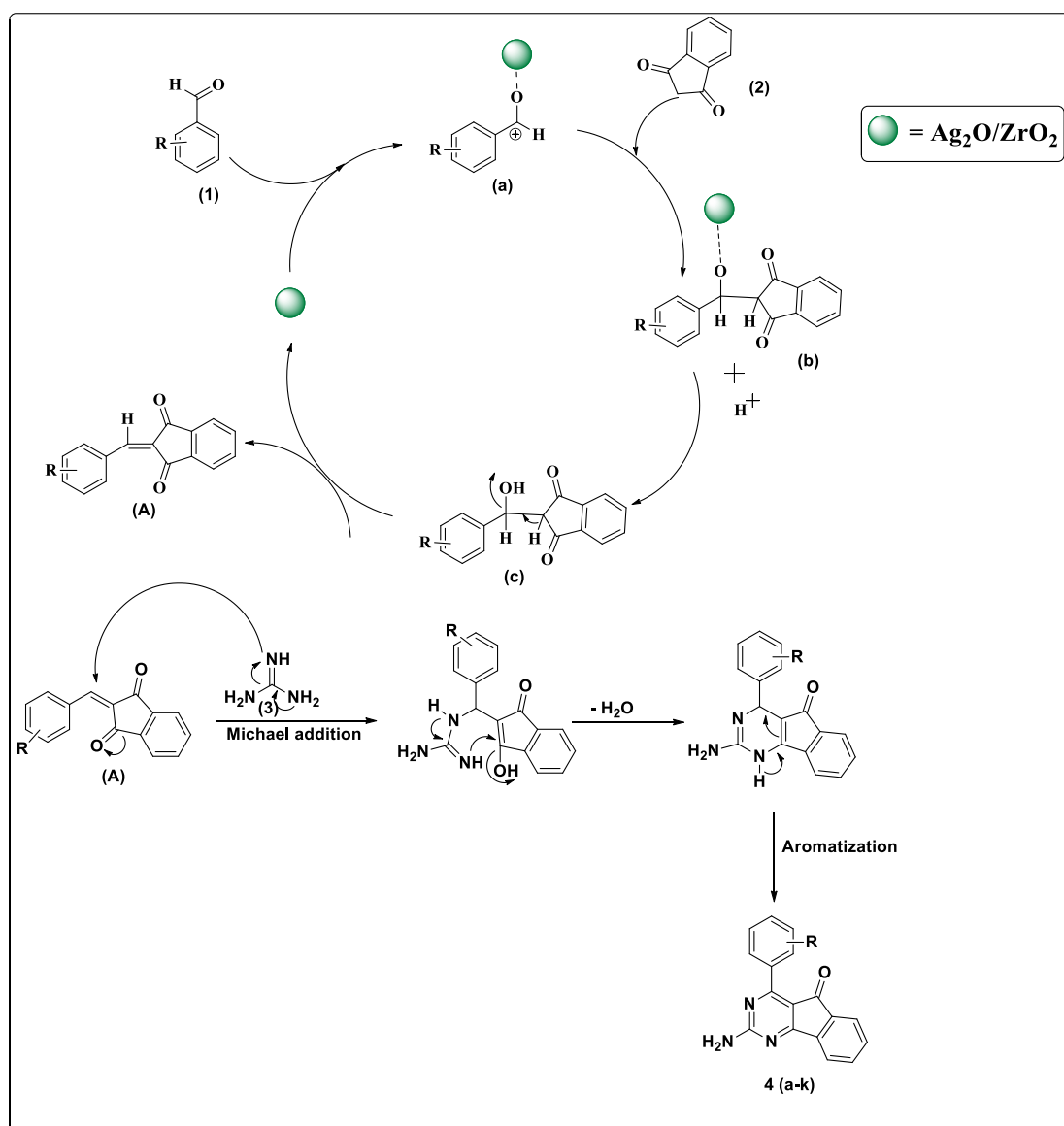

Scheme 2. Probable mechanism for the synthesis of novel indenopyrimidine derivatives.

Table 5. A comparison table with various other catalysts for synthesizing pyrimidine derivatives.

Catalyst	Solvent	Reaction Condition	Yield (%) [Ref]
NaOH	EtOH	Reflux, 6–10 h	81–94 [20]
NaOH	EtOH	Reflux, 7–8.4 h	75–86 [21]
NaOH	EtOH	Reflux, 0.5–1 h	85–94 [22]
NaOMe	EtOH	Reflux, 10–14 h	60–70 [23]
α-Fe$_2$O$_3$-MCM-41-P	Solvent free	80 °C, 1 h	82–95 [25]
Uranyl acetate/succinimide sulfonic acid	Solvent free	90 °C, 4 h	75–96 [26]
2.5% Ag$_2$O–ZrO$_2$	EtOH	RT, 30 min	90–96 [Present Work]

5. Reusability of Catalyst

The main objective and attraction of heterogeneous catalysts are its reusability. We thus examined the recovery and reusability of the Ag$_2$O/ZrO$_2$ catalyst. The solid catalyst from the reaction mixture was separated by simple filtration under vacuum, followed by washing with acetone solvent and drying at 100 °C for 3 h. The recovered catalyst was reused in subsequent reactions. Six runs in successive reactions gave yields without significant loss in product yield (Figure 6).
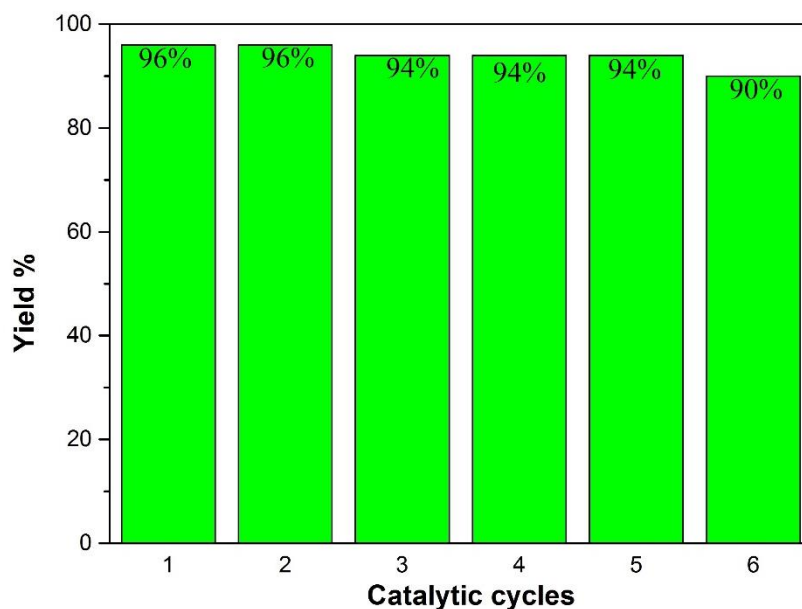
Figure 6. Recyclability of the Ag$_2$O/ZrO$_2$ catalyst.

6. Conclusions

In conclusion, we report a simple and green protocol for the synthesis of indenopyrimidines by a three-component reaction. All the reactions involving the reaction of 11 different aromatic aldehydes with 1,3-indandione and guanidinium hydrochloride using (2.5%) silver loaded on a zirconia catalyst gave excellent yields (90–96%). The proposed catalyst proved efficient, stable, and reusable. This method offers easy workup, excellent selectivity, and high yields in short reaction times at room temperature using ethanol, a green solvent. All the products were purified by recrystallization from ethanol. This method needs no chromatographic separation. Consequently, the use of volatile and hazardous solvents has been evaded. This method is useful for synthesizing various privileged pyrimidine scaffolds in short times in a one-pot strategy under green conditions.

Author Contributions: V.H.S.S.B. and S.M. conceived and designed the experiments; V.H.S.S.B. performed the experiments; V.H.S.S.B., S.M., W.V.Z., and S.B.J. analyzed the data; V.H.S.S.B., S.M., W.V.Z., and S.B.J. wrote the paper. All authors read and approved the final manuscript.

Conflicts of Interest: The authors declare no conflict of interest.

References

1. Rotstein, B.H.; Zaretsky, S.; Rai, V.; Yudin, A.K. Small heterocycles in multicomponent reactions. *Chem. Rev.* **2014**, *114*, 8323–8359. [CrossRef] [PubMed]

2. Domling, A.; Wang, W.; Wang, K. Chemistry and biology of multicomponent reactions. *Chem. Rev.* **2012**, *112*, 3083–3135. [CrossRef] [PubMed]

3. Gangu, K.K.; Maddila, S.; Maddila, S.N.; Jonnalagadda, S.B. Novel iron doped calcium oxalates as promising heterogeneous catalysts for one-pot multi-component synthesis of pyranopyrazoles. *RSC Adv.* **2017**, *7*, 423–432. [CrossRef]

4. Bhaskaruni, S.V.H.S.; Maddila, S.; Gangu, K.K.; Jonnalagadda, S.B. A review on multi-component green synthesis of N-containing heterocycles using mixed oxides as heterogeneous catalysts. *Arab. J. Chem.* **2017**. [CrossRef]

5. Bhaskaruni, S.V.H.S.; Maddila, S.; van Zyl, W.E.; Jonnalagadda, S.B. RuO_2/ZrO_2 as an efficient reusable catalyst for the facile, green, one-pot synthesis of novel functionalized halopyridine derivatives. *Catal. Commun.* **2017**, *100*, 24–28. [CrossRef]

6. Pagadala, R.; Maddila, S.; Moodley, V.; van Zyl, W.E.; Jonnalagadda, S.B. An efficient method for the multicomponent synthesis of multisubstituted pyridines, a rapid procedure using Au/MgO as the catalyst. *Tetrahedron Lett.* **2014**, *55*, 4006–4010. [CrossRef]

7. Bhaskaruni, S.V.H.S.; Maddila, S.; van Zyl, W.E.; Jonnalagadda, S.B. V_2O_5/ZrO_2 as an efficient reusable catalyst for the facile, green, one-pot synthesis of novel functionalized 1,4-dihydropyridine derivatives. *Catal. Today* **2017**. [CrossRef]

8. Maddila, S.N.; Maddila, S.; van Zyl, W.E.; Jonnalagadda, S.B. Mn doped ZrO_2 as a green, efficient and reusable heterogeneous catalyst for the multicomponent synthesis of pyrano[2,3-D]-pyrimidine derivatives. *RSC Adv.* **2015**, *5*, 37360–37366. [CrossRef]

9. Wen, C.; Yin, A.; Dai, W.-L. Recent advances in silver-based heterogeneous catalysts for green chemistry processes. *Appl. Catal. B Environ.* **2014**, *160–161*, 730–741. [CrossRef]

10. Maddila, S.; Jonnalagadda, S.B.; Gangu, K.K.; Maddila, S.N. Recent Advances in the Synthesis of Pyrazole Derivatives Using Multicomponent Reactions. *Curr. Org. Synth.* **2017**, *14*, 634–653. [CrossRef]

11. Gore, R.P.; Rajput, A.P. A review on recent progress in multicomponent reactions of pyrimidine synthesis. *Drug Invent. Today* **2013**, *5*, 148–152. [CrossRef]

12. Yalagala, K.; Maddila, S.; Rana, S.; Maddila, S.N.; Kalva, S.; Skelton, A.A.; Jonnalagadda, S.B. Synthesis, antimicrobial activity and molecular docking studies of pyrano[2,3-D]pyrimidine formimidate derivatives. *Res. Chem. Intermed.* **2016**, *42*, 3763–3774. [CrossRef]

13. Maddila, S.; Gorle, S.; Seshadri, N.; Lavanya, P.; Jonnalagadda, S.B. Synthesis, antibacterial and antifungal activity of novel benzothiazole pyrimidine derivatives. *Arab. J. Chem.* **2016**, *9*, 681–687. [CrossRef]

14. Raić-Malić, S.; Svedružić, D.; Gazivoda, T.; Marunović, A.; Hergold-Brundić, A.; Nagl, A.; Balzarini, J.; De Clercq, E.; Mintas, M. Synthesis and Antitumor Activities of Novel Pyrimidine Derivatives of 2,3-*O*,*O*-Dibenzyl-6-deoxy-L-ascorbic Acid and 4,5-Didehydro-5,6-dideoxy-L-ascorbic Acid. *J. Med. Chem.* **2000**, *43*, 4806–4811. [CrossRef] [PubMed]

15. Miazga, A.; Ziemkowski, P.; Siwecka, M.A.; Lipniacki, A.; Piasek, A.; Kulikowski, T. Synthesis, biological properties and anti-HIV-1 activity of new pyrimidine P1,P2-dinucleotides. *Nucleosides Nucleotides Nucleic Acids* **2010**, *29*, 438–444. [CrossRef] [PubMed]

16. Yadlapalli, R.K.; Chourasia, O.P.; Vemuri, K.; Sritharan, M.; Perali, R.S. Synthesis and in vitro anticancer and antitubercular activity of diarylpyrazole ligated dihydropyrimidines possessing lipophilic carbamoyl group. *Bioorg. Med. Chem. Lett.* **2012**, *22*, 2708–2711. [CrossRef] [PubMed]

17. De Assis, S.P.O.; da Silva, M.T.; de Oliveira, R.N.; de Lima, V.L.M. Synthesis and Anti-Inflammatory Activity of New Alkyl-Substituted Phthalimide 1*H*-1,2,3-Triazole Derivatives. *Sci. World J.* **2012**, *2012*, 925925. [CrossRef] [PubMed]

18. Singh, K.; Kaur, T. Pyrimidine-based antimalarials: Design strategies and antiplasmodial effects. *Medchemcomm* **2016**, *7*, 749–768. [CrossRef]

19. Lim, H.-K.; Chen, J.; Sensenhauser, C.; Cook, K.; Preston, R.; Thomas, T.; Shook, B.; Jackson, P.F.; Rassnick, S.; Rhodes, K.; et al. Overcoming the Genotoxicity of a Pyrrolidine Substituted Arylindenopyrimidine As a Potent Dual Adenosine A2A/A1 Antagonist by Minimizing Bioactivation to an Iminium Ion Reactive Intermediate. *Chem. Res. Toxicol.* **2011**, *24*, 1012–1030. [CrossRef] [PubMed]

20. Patravale, A.A.; Gore, A.H.; Patil, D.R.; Kolekar, G.B.; Deshmukh, M.B.; Anbhule, P.V. Trouble-Free Multicomponent Method for Combinatorial Synthesis of 2-Amino-4-phenyl-5-*H*-indeno[1,2-*d*]pyrimidine-5-one and Their Screening against Cancer Cell Lines. *Ind. Eng. Chem. Res.* **2014**, *53*, 16568–16578. [CrossRef]

21. Undare, S.S.; Valekar, N.J.; Patravale, A.A.; Jamale, D.K.; Vibhute, S.S.; Walekar, L.S.; Kolekar, G.B.; Deshmukh, M.B.; Anbhule, P.V. Synthesis, anti-inflammatory, ulcerogenic and cyclooxygenase activities of indenopyrimidine derivatives. *Bioorg. Med. Chem. Lett.* **2016**, *26*, 814–818. [CrossRef] [PubMed]

22. Xia, S.; Yin, S.; Tao, S.; Shi, Y.; Rong, L.; Wei, X.; Zong, Z. An efficient and facile synthesis of novel substituted pyrimidine derivatives: 4-amino-5-carbonitrile-2-nitroaminopyrimidine. *Res. Chem. Intermed.* **2012**, *38*, 2435–2442. [CrossRef]

23. Jagadale, S.D.; Sawant, A.D.; Deshmukh, M.B. Synthesis and Antimicrobial Evaluation of Novel Dibenzo-18-Crown-6-Ether Functionalized Pyrimidines. *J. Heterocycl. Chem.* **2017**, *54*, 2307–2312. [CrossRef]

24. Gogoi, P.; Dutta, A.K.; Saikia, S.; Borah, R. Heterogenized hybrid catalyst of 1-sulfonic acid-3-methyl imidazolium ferric chloride over NaY zeolite for one-pot synthesis of 2-amino-4-arylpyrimidine derivatives: A viable approach. *Appl. Catal. A Gen.* **2016**, *523*, 321–331. [CrossRef]

25. Aryan, R.; Beyzaei, H.; Nojavan, M.; Dianatipour, T. Secondary amines immobilized inside magnetic mesoporous materials as a recyclable basic and oxidative heterogeneous nanocatalyst for the synthesis of trisubstituted pyrimidine derivatives. *Res. Chem. Intermed.* **2016**, *42*, 4417–4431. [CrossRef]

26. Kamali, M.; Shockravi, A.; Doost, M.S.; Hooshmand, S.E. One-pot, solvent-free synthesis via Biginelli reaction: Catalyst-free and new recyclable catalysts. *Cogent Chem.* **2015**, *24*, 1–6. [CrossRef]

27. Zhang, J.; Li, L.; Wang, S.; Huang, T.; Hao, Y.; Qi, Y. Multi-mode photocatalytic degradation and photocatalytic hydrogen evolution of honeycomb-like three-dimensionally ordered macroporous composite Ag/ZrO$_2$. *RSC Adv.* **2016**, *6*, 13991–14001. [CrossRef]

28. Lee, C.; Shul, Y.-G.; Einaga, H. Silver and manganese oxide catalysts supported on mesoporous ZrO$_2$ nanofiber mats for catalytic removal of benzene and diesel soot. *Catal. Today* **2017**, *281*, 460–466. [CrossRef]

29. Shabalala, N.G.; Maddila, S.; Jonnalagadda, S.B. Facile one-pot green synthesis of tetrahydrobiphenylene-1, 3-dicarbonitriles in aqueous media under ultrasound irradiation. *Res. Chem. Intermed.* **2016**, *42*, 8097–8108. [CrossRef]

30. Shabalala, N.; Maddila, S.; Jonnalagadda, S.B. Catalyst-free, one-pot, four-component green synthesis of functionalized 1-(2-fluorophenyl)-1,4-dihydropyridines under ultrasound irradiation. *New J. Chem.* **2016**, *40*, 5107–5112. [CrossRef]

31. Shabalala, S.; Maddila, S.; van Zyl, W.E.; Jonnalagadda, S.B. Sustainable CeO$_2$/ZrO$_2$ Mixed Oxide Catalyst For the Green Synthesis of Highly Functionalized 1,4-Dihydropyridine-2,3-dicarboxylate Derivatives. *Curr. Org. Synth.* **2017**, *14*, 1–8. [CrossRef]

32. Shabalala, S.; Maddila, S.; van Zyl, W.E.; Jonnalagadda, S.B. Innovative Efficient Method for the Synthesis of 1,4-Dihydropyridines Using Y$_2$O$_3$ Loaded on ZrO$_2$ as Catalyst. *Ind. Eng. Chem. Res.* **2017**, *56*, 11372–11379. [CrossRef]

33. Gangu, K.K.; Maddila, S.; Maddila, S.N.; Jonnalagadda, S.B. Nanostructured samarium doped fluorapatites and their catalytic activity towards synthesis of 1,2,4-triazoles. *Molecules* **2016**, *21*, 1281. [CrossRef] [PubMed]

34. Maddila, S.; Lavanya, P.; Jonnalagadda, S.B. Cesium loaded on silica as an efficient and recyclable catalyst for the novel synthesis of selenophenes. *Arab. J. Chem.* **2016**, *9*, 891–897. [CrossRef]

35. Maddila, S.; Valand, J.; Bandaru, H.; Yalagala, K.; Lavanya, P. Ag Loaded on SiO$_2$ as an Efficient and Recyclable Heterogeneous Catalyst for the Synthesis of Chloro-8-substituted-9H-purines. *J. Heterocycl. Chem.* **2016**, *53*, 319–324. [CrossRef]

36. Maddila, S.; Maddila, S.N.; Jonnalagadda, S.B.; Lavanya, P. Reusable Ce-V Loaded Alumina Catalyst for Multicomponent Synthesis of Substituted Pyridines in Green Media. *J. Heterocycl. Chem.* **2016**, *53*, 658–664. [CrossRef]

37. Maddila, S.; Gorle, S.; Shabalala, S.; Oyetade, O.; Maddila, S.N.; Lavanya, P.; Jonnalagadda, S.B. Ultrasound mediated green synthesis of pyrano[2,3-*c*]pyrazoles by using Mn doped ZrO$_2$. *Arab. J. Chem.* **2016**. [CrossRef]

38. Maddila, S.; Dasireddy, V.D.B.C.; Jonnalagadda, S.B. Ce-V loaded metal oxides as catalysts for dechlorination of chloronitrophenol by ozone. *Appl. Catal. B Environ.* **2014**, *150–151*, 305–314. [CrossRef]

39. Maddila, S.; Dasireddy, V.D.B.C.; Jonnalagadda, S.B. Dechlorination of tetrachloro-o-benzoquinone by ozonation catalyzed by cesium loaded metal oxides. *Appl. Catal. B Environ.* **2013**, *138–139*, 149–160. [CrossRef]

40. Balaga, V.; Pedada, J.; Friedrich, H.B.; Singh, S. Tuning surface composition of Cs exchanged phosphomolybdic acid catalysts in CH bond activation of toluene to benzaldehyde at room temperature. *J. Mol. Catal. A Chem.* **2016**, *425*, 116–123. [CrossRef]

41. Védrine, J.C. Acid-base characterization of heterogeneous catalysts: An up-to-date overview. *Res. Chem. Intermed.* **2015**, *41*, 9387–9423. [CrossRef]

42. Li, Q.; Wang, X.; Yu, Y.; Chen, Y.; Dai, L. Tailoring a magnetically separable NiFe$_2$O$_4$ nanoparticle catalyst for Knoevenagel condensation. *Tetrahedron* **2016**, *72*, 8358–8363. [CrossRef]

Sample Availability: Samples of the compounds are available from the authors.